

Validation of Multitemperature Nozzle Flow Code

Chul Park*

NASA Ames Research Center, Moffett Field, California 94035
and

Seung-Ho Lee†

Eloret Institute, Palo Alto, California 94303

A computer code nozzle in n -temperatures (NOZNT), which calculates one-dimensional flows of partially dissociated and ionized air in an expanding nozzle, is tested against three existing sets of experimental data taken in arcjet wind tunnels. The code accounts for the differences among various temperatures, i.e., translational-rotational temperature, vibrational temperatures of individual molecular species, and electron-electronic temperature, and the effects of impurities. The experimental data considered are 1) the spectroscopic emission data, 2) electron beam data on vibrational temperature, and 3) mass-spectrometric species concentration data. It is shown that the impurities are inconsequential for the arcjet flows, and the NOZNT code is validated by numerically reproducing the experimental data.

Nomenclature

- A = cross-sectional area of nozzle, m^2
 C = reaction rate constant, $\text{cm}^3 \text{mole}^{-1} \text{s}^{-1}$, Eq. (1)
 E_{vi} = vibrational energy of species i , J/kg
 H = enthalpy, J/kg
 k_f = forward reaction rate coefficient, $\text{cm}^3/(\text{mole-s})$
 k_r = reverse reaction rate coefficient, $\text{cm}^3/(\text{mole-s})$
 or $\text{cm}^6/(\text{mole}^2\text{-s})$
 M = unspecified third body in dissociation
 n = pre-exponential temperature power, Eq. (1)
 P = probability for vibration-vibration energy transfer
 p = pressure, atm
 R = gas constant, J/(kg-K)
 S = entropy, J/(kg-K)
 T = translational-rotational temperature, K
 T_d = characteristic reaction temperature, K
 T_e = electron-electronic temperature, K
 T_f = temperature controlling forward rate, K
 T_r = temperature controlling reverse rate, K
 T_{vi} = vibrational temperature of species i , K
 T_x = temperature controlling a reaction, K
 x = distance from throat, m
 σ_{ev} = vibration-electronic energy transfer cross section, cm^2
 σ_{iv} = cross section for energy transfer between vibrational modes of different molecules, cm^2
 τ_e = electron-thermal to vibration relaxation time, s
 τ_{MW} = vibrational relaxation time of Millikan and White, s
 T_{vi} = heavy-particle translational to vibrational relaxation time for species i , s
 ϕ = ratio of the vibrational relaxation time behind a shock to that in expanding flow

Subscripts

- e = electron-electronic
 i = species index
 s = settling chamber
 $*$ = throat

Introduction

It has been known for several decades that a high-enthalpy gas flow expanding through the nozzle of a high-enthalpy wind tunnel exhibits thermal and chemical nonequilibrium phenomena. The nonequilibrium phenomena cause several undesirable effects in the testing of models in such a wind tunnel. The first well-known nonequilibrium phenomenon concerns vibrational excitation, studied in some depth in Ref. 1. Simple correlation formulas for the so-called vibrational relaxation time τ_v , were devised in Ref. 2 by which the relaxation times for a flow with little or no dissociation can be calculated. The correlation formula is invalid if the gas is NO ,³ or if the gas contains atomic oxygen.⁴⁻⁶

Considerable efforts have been made to experimentally determine whether the vibrational temperature behaves in an expanding flow as predicted by the τ_v values derived from the shock wave experiments.⁷⁻¹⁴ Results of such experiments seemed to indicate that vibrational relaxation in an expanding flow occurs at a rate faster than behind a shock wave.^{7,8,13,14} The studies led to the introduction of a quantity ϕ that represents the ratio of the relaxation rate in an expanding flow to that behind a shock wave. It was generally agreed in those early studies that ϕ is nearly unity if the colliding species is argon,⁹ about 3 for CO colliding with CO,¹⁰ and a value much larger than 3 if the gas is air^{7,13} or contains impurities.^{7,11} Recent theoretical studies of Ruffin and Park,¹² and experimental studies by Sharma and his associates,^{15,16} show that ϕ is no more than 1.5 for pure N_2 for the relaxation of vibrational energy and the average (energy-averaged) vibrational temperature corresponding to the vibrational energy. However, the vibrational temperature defined by the distribution of the low vibrational states is generally lower than the average vibrational temperature because of the so-called Treanor distribution among them.^{17,18} The magnitude of the difference between the two vibrational temperatures depends on the extent of prevalence of the Treanor distribution.

The second well-known nonequilibrium phenomenon in a diatomic gas concerns freezing of atomic recombination processes.¹⁹ Despite the prominence of this theory, very little experimental measurements have ever been made to date to

Presented as Paper 93-2862 at the AIAA 28th Thermophysics Conference, Orlando, FL, July 6–9, 1993; received Aug. 12, 1993; revision received April 29, 1994; accepted for publication July 7, 1994. Copyright © 1994 by the American Institute of Aeronautics and Astronautics, Inc. No copyright is asserted in the United States under Title 17, U.S. Code. The U.S. Government has a royalty-free license to exercise all rights under the copyright claimed herein for Governmental purposes. All other rights are reserved by the copyright owner.

*Senior Staff Scientist. Associate Fellow AIAA.

†Research Scientist (deceased). Member AIAA.

confirm it. The only systematic study was made by MacDermott et al.,^{20,21} who measured the species concentrations in the test section of an arcjet wind tunnel using a mass spectrometer. Their work showed that the measured species concentrations did not agree with those calculated using the then best-available technique. The measured concentration of atomic oxygen was smaller, and that of atomic nitrogen was very much larger than predicted. One could further cite the indirect verification of the freezing phenomenon, such as the work in Ref. 22, in which the angle of the oblique shock wave formed over a wedge is measured. Because the shock angle is related to the amount of chemical energy contained in the freestream, the shock angle could be an indicator of the nonequilibrium state in the freestream. However, such measurements cannot be said to be definitive because of the uncertainty associated with the nonequilibrium flow process behind a shock wave.²³

Independently, electron number density and electron temperature have been measured in diatomic gases by Dunn and Lordi.^{24–26} Their works showed that electron temperature is considerably higher than the heavy-particle translational temperature. Electrons cool rapidly along the nozzle if the flow contains oxygen. A theory has been postulated to explain this behavior,²⁷ but has not yet been tested quantitatively against the experimental data. Very recently, a spectroscopic emission measurement of the vibrational and electronic temperatures has been made of the stream produced in an arcjet wind tunnel.²⁸ The result obtained shows that the electronic temperature is considerably higher than the vibrational temperature of NO.

To complicate the problem even further, theoretical prediction has been made recently that a finite, though small, amount of energy, called "hidden energy," may be contained in the highly excited vibrational and rotational modes in an expanding flow that has never been accounted for previously.²⁹

Thus, the problem of nonequilibrium in an expanding flow is at best very poorly understood. Existing experimental data disagree with theoretical predictions, or have not yet been explained fully. It is the purpose of the present work to explain the existing experimental data, and through the process, to produce a tool by which the nozzle flow behavior can be correctly calculated.

The effort centers around a newly developed code named NOZNT (nozzle in *n*-temperatures). The code is a modification of NOZ3T introduced in Ref. 29. In NOZNT, assumption is made as in NOZ3T that the rotational temperature of the molecules is equal to the heavy-particle translational temperature T , and the electronic excitation temperature is equal to the electron translational temperature T_e . However, unlike NOZ3T, the vibrational temperatures of the individual species i , T_{vi} , are taken to be in general different from each other, as well as from T and T_e . The vibrational temperatures are the energy-averaged temperatures, which relaxes according to the known relaxation rates.¹⁸ The temperatures T_{vi} and T_e are calculated by integrating the governing rate equations accounting for vibration-to-translation, vibration-to-vibration, vibration-to-electron thermal, and vibration-to-electronic energy transfer mechanisms, and radiative cooling. All processes affecting electron-electronic energies considered in Ref. 27 are accounted for in the code. The recent results of Sharma et al.¹⁵ and Gillespie et al.¹⁶ are used as the basis for calculating vibrational temperatures. Attention is given to the possible effects of impurity species in the flow. The calculation was performed to numerically recreate the three sets of experimental data taken in arcjet wind tunnels: 1) the spectral emission measurement,²⁸ 2) the electron beam measurement of vibrational temperature,¹³ and 3) the mass spectrometric measurement of species concentrations.^{20,21}

The present work shows that by using the available information on rate parameters, and selecting some of the unknown rate parameters appropriately, the three sets of ex-

perimental data can be reproduced fairly closely using the NOZNT code. The vibrational relaxation occurs at the same rate in an expanding flow as behind a shock wave as found by Sharma and his associates,^{12,15,16} and the low observed atomic oxygen concentration and high observed atomic nitrogen concentration are attributable to the enhanced rates of NO exchange reactions caused by the high electronic temperature of the species involved.

Method

Flow Equations

The computer code NOZNT solves a one-dimensional steady flow through a convergent-divergent nozzle in the dissociated and ionized regime. Equilibrium is assumed at the entrance of the nozzle. The early portion of the nozzle flow is solved assuming equilibrium, to an arbitrary point, either upstream or downstream of throat, specified by the user. The flow downstream of this point is solved assuming multitemperature nonequilibrium as mentioned above. The various temperatures enter into determination of the rate coefficients as described later. Except for those specified below, the basic thermochemical model used is the same as those in Ref. 30. Additionally, a variation of NOZNT, NOZ1T, is developed in order to calculate the flow assuming all temperatures to be the same, for the purpose of comparison. The basic formulation is the same as in the standard nonequilibrium flow calculation method such as that in Ref. 31. The so-called hidden vibrational and rotational energies postulated in Ref. 29 is neglected because it is very small.

Nozzle geometry is determined by specifying the area ratios A/A_* at three points $x = x_1, x_2$, and x_3 , where x is measured from the throat. A combination of hyperbola and parabola is used to produce a smoothly varying area change with a non-negative dA/dx at the exit. For all example calculations presented in the present work, nozzle geometry is assumed to be hyperbolic, i.e., conical with a smooth transition at throat, of the form $A/A_* = 1 + cx^2$, and the nonequilibrium calculation is initiated at a point early upstream of the throat.

The equations are solved by marching in space using the implicit integrating scheme of Ref. 32. In that scheme, spatial step sizes are automatically adjusted to limit errors to within a given tolerance. The tolerance is set through trial and error to a value below which the solution no longer depends on it.

Reaction Rates for Air

General

In a multitemperature environment, one expresses the reaction rate coefficients in the form³⁰

$$k_f = CT_x^n \exp(-T_d/T_x) \quad (1)$$

The unspecified temperature T_x is designated as T_f in a forward (endothermic) reaction, and as T_r in a reverse (exothermic) reaction.

Atomic Recombination Reactions

In an expanding flow under study, the predominant reaction is atomic recombination, for which vibrational temperature is not involved. Therefore, the temperature in control of dissociation/recombination processes for an expanding flow is the translational-rotational temperature T , $T_r = T$. T_f is set also to T for the sake of simplicity for atomic recombination processes.

There exist in the literature many sets of reaction rate parameters C and n chosen for air. Three sets of the parameters are considered in the present work: 1) those of Park,³⁰ 2) Lordi et al.,³¹ and 3) the National Aero-Space Plane (NASP) Committee.³³ The set by Lordi et al. is referred to here as NENZF set because it was used in the computer code nonequilibrium nozzle flow (NENZF).³¹ The NASP set provides the parameters only for $M = \text{Ar}$ (argon). Park's rate coef-

Table 1 Reaction rate coefficients for air (C is in $\text{cm}^3\text{mol}^{-1}\text{s}^{-1}$)

Reaction	M	T_f	T_r	C	n	T_d	Ref.
Dissociation reactions							
$\text{N}_2 + \text{M} \rightarrow \text{N} + \text{N} + \text{M}$	N	T	T	3.0^{22}	-1.6	113,200	30
	O	—	—	3.0^{22}	—	—	—
	N_2	—	—	7.0^{21}	—	—	—
	O_2	—	—	7.0^{21}	—	—	—
	NO	—	—	7.0^{21}	—	—	—
	e	T_e	T_e	1.2^{25}	—	—	36
$\text{O}_2 + \text{M} \rightarrow \text{O} + \text{O} + \text{M}$	N	T	T	1.0^{22}	-1.5	59,500	30
	O	—	—	1.0^{22}	—	—	—
	N_2	—	—	2.0^{21}	—	—	—
	O_2	—	—	2.0^{21}	—	—	—
	NO	—	—	2.0^{21}	—	—	—
$\text{NO} + \text{M} \rightarrow \text{O} + \text{O} + \text{M}$	N	T	T	1.1^{17}	0.0	75,500	30
	O	—	—	1.1^{17}	—	—	—
	N_2	—	—	5.0^{15}	—	—	—
	O_2	—	—	5.0^{15}	—	—	—
	NO	—	—	1.1^{17}	—	—	—
Neutral exchange reactions							
$\text{N}_2 + \text{O} \rightarrow \text{NO} + \text{N}$	—	T_e	T	1.8^{14}	0.0	38,400	35
$\text{NO} + \text{O} \rightarrow \text{O}_2 + \text{N}$	—	$T_v^{0.1} T_e^{0.9}$	T	2.4^9	1.0	19,220	35
Associative ionization reactions							
$\text{N} + \text{O} \rightarrow \text{NO}^+ + \text{e}$	—	T	T_e	8.8^8	1.0	31,900	36
$\text{O} + \text{O} \rightarrow \text{O}_2^+ + \text{e}$	—	T	T_e	7.1^{12}	2.7	80,600	36
$\text{N} + \text{N} \rightarrow \text{N}_2^+ + \text{e}$	—	T	T_e	4.4^7	1.5	67,500	36
Electron-impact ionization reactions							
$\text{O} + \text{e} \rightarrow \text{O}^+ + \text{e} + \text{e}$	—	T_e	T_e	3.9^{33}	-3.78	158,500	30
$\text{N} + \text{e} \rightarrow \text{N}^+ + \text{e} + \text{e}$	—	T_e	T_e	2.5^{34}	-3.82	168,600	30
$\text{Cu} + \text{e} \rightarrow \text{Cu}^+ + \text{e} + \text{e}$	—	T_e	T_e	8.6^{34}	-3.62	89,640	^a
$\text{Ar} + \text{e} \rightarrow \text{Ar}^+ + \text{e} + \text{e}$	—	T_e	T_e	2.3^{34}	-3.60	182,890	^a
Radiative recombination reactions							
$\text{O} + h\nu \leftarrow \text{O}^+ + \text{e}$	—	T_e	—	1.1^{12}	-0.52	—	36
$\text{N} + h\nu \leftarrow \text{N}^+ + \text{e}$	—	T_e	—	1.5^{12}	-0.48	—	36
$\text{Cu} + h\nu \leftarrow \text{Cu}^+ + \text{e}$	—	T_e	—	1.5^{12}	-0.48	—	^b

^aReverse rate assumed to be the same as for $\text{N} + \text{e} \rightarrow \text{N}^+ + \text{e} + \text{e}$. ^bAssumed to be the same as for $\text{N}^+ + \text{e} \rightarrow \text{N} + h\nu$.

ficient values are slightly higher than the NENZF values for oxygen dissociation/recombination. The $M = \text{Ar}$ value for NASP set is considerably smaller than the other two. In the present work, Park's set is selected because, as will be shown later, it best reproduces the experimental data.

Exchange Reactions

The two NO exchange reactions



are substantially endothermic. Therefore, forward rates are expected to be fast if the oxygen atom appearing as a reactant on the left side is electronically excited to its 1D state. There are many reactions in which $\text{O}(^1D)$ is known to accelerate reactions (e.g., Ref. 34). In addition, if the reactant molecules, N_2 and NO, are vibrationally excited, the forward reactions will occur faster. Therefore, T_f for this reaction should be a function of T_e and T_v . The weight of T_e should be greater for reactions of greater endothermicity. Reaction (2) has a relatively large endothermicity of 315 KJ/mol. For the reason to become apparent later, we set for this reaction

$$(\text{N}_2 + \text{O} \rightarrow \text{NO} + \text{O}) \quad T_f = T_e \quad (4)$$

Reaction (3) has a smaller endothermicity of 133 KJ/mol. For this reaction, we set

$$(\text{NO} + \text{O} \rightarrow \text{O}_2 + \text{N}) \quad T_f = T_v^{0.1} T_e^{0.9} \quad (5)$$

The choices of T_f made in Eqs. (4) and (5) will be discussed further in the Discussion.

For the reverse rates of the NO exchange reactions, electronic or vibrational excitation of reactants is immaterial be-

cause the rates are exothermic. Therefore, T_r for both reactions (2) and (3) is taken to be T . The C and n values for these reactions are taken from the work of Hanson and Similian.³⁵

The rate parameters adopted in the present work for reactions (2) and (3) are the same as those in the NASP set. The selected rate coefficients are the same as those adopted by Park^{30,36} at 4000 K. However, there exists a considerable difference between the Park/NASP set and the NENZF set, especially for reaction (3).

Ionic Reactions

For the electron-impact ionization and ionic recombination process $\text{X} + \text{e} \rightleftharpoons \text{X}^+ + \text{e} + \text{e}$, rate coefficients are given in Ref. 30 for N and O. Electron temperature T_e is the controlling temperature for both k_f and k_r for this process. The rate coefficients for the radiative recombination reactions of the form $\text{X} + h\nu \leftarrow \text{X}^+ + \text{e}$ are given also for N and O in Ref. 36. The radiative recombination of molecular ions, $\text{N}_2^+ + \text{e} \rightarrow \text{N}_2 + h\nu$, $\text{O}_2^+ + \text{e} \rightarrow \text{O}_2 + h\nu$, and $\text{NO}^+ + \text{e} \rightarrow \text{NO} + h\nu$ are neglected for the reason that they are negligibly slower than the competing dissociative recombination processes discussed below.

Associative Ionization/Dissociative Recombination

The rate coefficients for the dissociative recombination reactions $\text{N} + \text{N} \leftarrow \text{N}_2^+ + \text{e}$, $\text{O} + \text{O} \leftarrow \text{O}_2^+ + \text{e}$, and $\text{N} + \text{O} \leftarrow \text{NO}^+ + \text{e}$ have been determined in an expanding flow by Dunn and Lordi.²⁴⁻²⁶ They were reevaluated by Park in Ref. 30 using additional experimental data. They are re-evaluated again in Ref. 36. The values in Ref. 36 are used in the present work. The controlling temperature for the forward reactions (associative ionization) is T for these reactions, while T_e is the controlling temperature for the reverse reactions.

The controlling temperatures, the values of C and n for all reactions considered, and their sources, are summarized in Table 1.

Excitation Rates for Air

Vibration-Translation Coupling

As mentioned in the Introduction, the vibrational temperatures used in the present work are the energy-averaged temperatures. The Millikan-White values of vibrational relaxation times will be denoted here by the symbol τ_{MW} . The formula requires two parameters a and b that are functions of the molecular constants. Millikan and White have shown that these parameters can be expressed for many gases by the simple expressions given in Ref. 2. For the cases where the molecule is NO or the colliding species is an atom, existing experimental data³⁻⁶ show that Millikan-White's expressions for a and b severely overestimate the relaxation time.³⁶ The a and b values for these exceptional cases are determined in Ref. 36 from the existing experimental data. In the present work, the a and b values recommended in Ref. 36 are used.

As mentioned in the Introduction, in an expanding flow, τ_{MW} value must be divided by a factor ϕ , which is in general larger than unity, i.e.,

$$\tau_{vi} = \tau_{MW,i}/\phi_i$$

The quantity ϕ is taken to be 1.5 for both N_2 and O_2 , the maximum possible value given to N_2 in Refs. 12, 15, and 16. For NO, it is taken to be 3, the value for CO.¹¹

Vibration-Vibration Coupling

The rates of vibrational energy transfer between different molecules are calculated from the experimental data of Ref. 37. The data are fitted in the present work using the energy transfer probability P of the form

$$(N_2 - NO) P = 5.5 \times 10^{-5} (T/1000)^{2.32}$$

$$(N_2 - O_2) P = 3 \times 10^{-6} (T/1000)^{2.87}$$

For the O_2 -NO encounters for which data are lacking, the P value is taken to be the same as for the N_2 -NO encounters. The cross section for energy transfer between the molecules i and j is calculated as $\sigma_{vi} = 10^{-15} P \text{ cm}^2$.

Vibration-Electron Coupling

The coupling between the electron translation and vibration is calculated for N_2 using the work of Lee.³⁸ For O_2 and NO, the same equation is used by shifting the effective electron temperature by the ratios of characteristic vibrational energies of the respective molecules, and by multiplying them by 300. This leads to

$$\tau_{e,O_2}(T_e) = 300 \times \tau_{e,N_2}(1.492T_e)$$

$$\tau_{e,NO}(T_e) = 300 \times \tau_{e,N_2}(1.239T_e)$$

The factor 300 accounts for the fact that the electron-vibration energy transfer cross sections for O_2 and NO are approximately that much smaller than those for N_2 .³⁹

Impurities

Origin of Impurities

In an arcjet wind tunnel, copper is introduced into the flow (e.g., Refs. 40 and 41), mostly from the electrodes. Therefore, a finite amount of copper is assumed to exist in the flow. The copper concentration is varied to investigate the effect of its presence.

Reaction Rates

When Cu interacts with oxygen, CuO can form. CuO has relatively low binding energies, i.e., 2.7 eV, and therefore

are unlikely to be produced in significant concentrations in the environment typical of an arcjet wind tunnel. The copper impurity has an ionization potential substantially lower than those of N or O. Therefore, it undergoes electron-impact ionization and recombination reactions $Cu + e \rightleftharpoons Cu^+ + e$, and radiative recombination $Cu + h\nu \leftarrow Cu^+ + e$ to a significant extent. Reference 42 shows that the recombination rate coefficients of all atoms are nearly the same. For this reason, the ionic reaction rate of Cu is selected in such a way that its reverse rate is the same as for nitrogen. The radiative recombination rate coefficient of copper is assumed to be the same as that for nitrogen for the same reason.

Vibrational Relaxation Parameters

Effects of metallic species on vibrational relaxation rate are unknown. However, it is suspected that these impurities enhance the vibrational relaxation rates greatly.⁷ To test this hypothesis, the vibrational relaxation times of N_2 , O_2 , and NO by the collisions with the impurity species Cu are given the shortest physically-possible times, that is, 3×10^{-9} s at 8000 K, and 4×10^{-9} s at 1000 K. This leads to $a = 5.753$ and $b = 0.2594$ for these species.

Results

Ames Arcjet Wind-Tunnel Flow

Gopaul et al.²⁸ at Ames Research Center determined the temperature(s) of the freestream flow in the test section of an arcjet wind tunnel from the radiation spectra emitted by the flow. For this experiment, p_s was 2.4 atm. The test gas was 90% air and 10% argon by volume. The mass-averaged flow enthalpy was 22 MJ/kg. The enthalpy at the centerline region of the test section, as determined from heat transfer rate measurement, was about 28 MJ/kg. The best agreement between the experimental and theoretical results is seen for the centerline enthalpy value of 30 MJ/kg.

According to the calculation, O_2 is almost totally dissociated in this flow environment. The concentration of NO^+ is negligibly small compared with those of N^+ and O^+ , and therefore can be neglected. The flow behavior is affected very little by the presence of copper, up to a concentration of several hundred ppm. The probable reason might be that the flow contains many free electrons, and so most of the electron-electronic energy is in the thermal mode of the electrons.

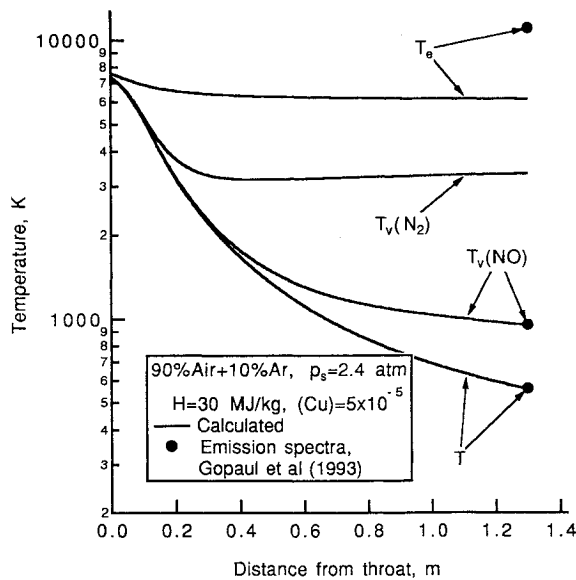
Emissions from the gamma and delta bands of NO molecules were measured spectrographically in the test section. Because the flow is hot only in the central core region of the flow, the observed emission is believed to emanate only from the core region. From the intensity pattern of the gamma band, rotational temperature T_r was determined to be about $T = 560$. From the fact that the radiation from the $v = 1$ state of the upper electronic state of the gamma band was absent, the vibrational temperature of NO, $T_v(NO)$, was determined to be less than 950. From the ratio of the intensity of the delta system to that of the gamma system, the electronic temperature is determined to be about 11,500 K. Since this was a single data point, the extent of error is unknown.

The experimental data are compared with the present calculation in Fig. 1. As seen in here, the vibrational temperatures of N_2 and NO differ greatly. The measured values of T and $T_v(NO)$ agree fairly well with the calculated values. However, the measured T_e is nearly twice the calculated value. The reason for this may be that the two electronic states, from the populations of which T_e is deduced, are not in equilibrium with the electron translation mode as assumed in the present model (see Discussion). However, the fact that the measured T_e is at least not equal to T or $T_v(NO)$ is an indication that a multitemperature approach is warranted.

Although not shown, the calculated vibrational temperature of NO was seen to be virtually unaffected by the choice of ϕ value: the ϕ value of 1.5 used for N_2 and O_2 leads to nearly identical results as the presently chosen value of 3.

Table 2 Operating conditions of the AEDC arcjet experiments and mole fractions at exit calculated by the present method

p_s , atm	T_s , K	S/R	H , MJ/kg	A/A^*	N, fraction	O, fraction	NO, fraction
15	2300	29.24	2.684	5000	3.62^{-8}	4.53^{-4}	1.51^{-2}
20	2300	29.02	2.684	5510	2.51^{-8}	3.89^{-4}	1.52^{-2}
10	3000	31.06	3.803	4180	4.17^{-5}	1.08^{-2}	4.27^{-2}
15	3000	30.68	3.780	4340	3.51^{-5}	7.74^{-3}	4.27^{-2}
20	3000	30.37	3.766	5040	3.17^{-5}	6.10^{-3}	4.28^{-2}
5	4000	34.46	6.771	2040	2.48^{-3}	1.33^{-1}	5.00^{-2}
10	4000	33.41	6.408	3330	1.87^{-3}	9.05^{-2}	5.84^{-2}
15	4000	32.83	6.224	3980	1.56^{-3}	6.70^{-2}	6.13^{-2}
20	4000	32.43	6.106	4410	1.49^{-3}	5.32^{-2}	6.38^{-2}
5	5000	37.03	9.669	1905	1.88^{-2}	2.35^{-1}	4.06^{-2}

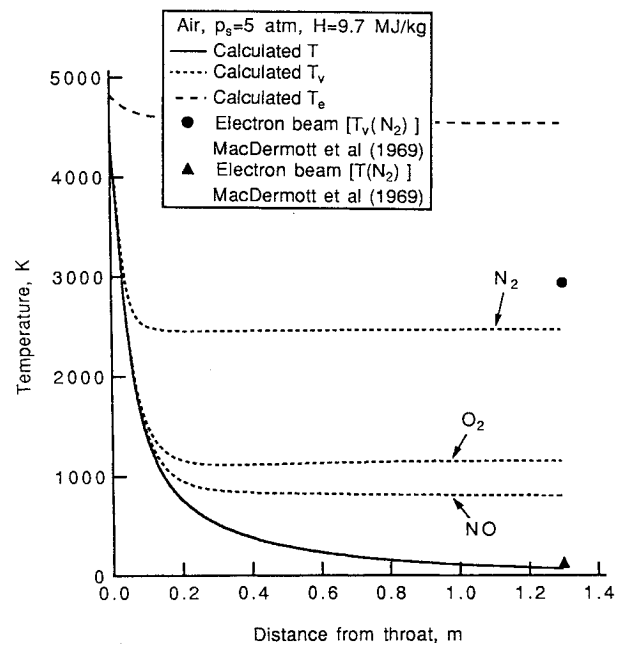
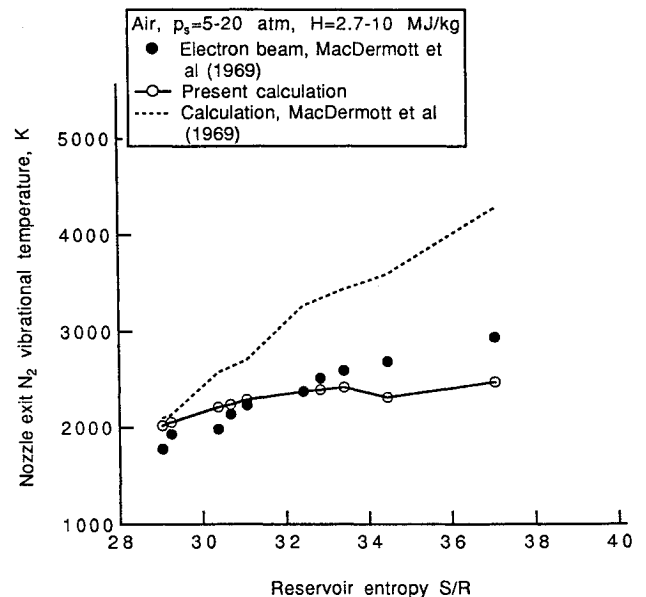
**Fig. 1** Comparison between the calculated and the measured temperatures along nozzle in air in an arcjet wind tunnel; measurement using emission spectroscopy.**AEDC Arcjet Vibrational Temperature Measurement**

Vibrational and rotational temperatures of N_2 were measured in an arcjet wind tunnel (18-in. Low Density Wind Tunnel) at AEDC by MacDermott et al.¹³ using an electron beam device. The operating conditions of the wind tunnel are presented in Ref. 13 in terms of the settling chamber pressure, temperature, and entropy S/R . The corresponding enthalpy values are presented in Table 2. The geometrical area ratio of the nozzle used in the experiment was about 8100. However, due to the viscous effects, the effective area ratio, deduced from the pitot impact measurements, varied between 1900–5500 as seen in the table.

As was the case with the arcjet flow in Ames' experiment, and as was concluded in Ref. 39, the flow behavior is affected little by copper. The calculation results shown here were carried out assuming copper concentration of 50 ppm by mole.

The calculated vibrational and rotational temperatures at the nozzle exit are compared with the experimental data for one case, the case of $p_s = 5$ atm and $H = 9.67$ MJ/kg, in Fig. 2. The extent of possible errors in the measurement has not been indicated in Ref. 13, and hence is presently unknown. The figure shows that the present calculation agrees with the experimental data to within about 15%.

In Fig. 3, the calculated vibrational temperatures at the nozzle are compared with the experimental data over the entire range of measurement. Shown also in the figure are the calculation by MacDermott et al.¹³ As seen here, the present calculation shows better agreement with the experimental data than MacDermott's calculation. The difference between the two calculations is mainly the effect of N_2 -O

**Fig. 2** Comparison between the calculated and the measured temperatures along nozzle in air in an arcjet wind tunnel; measurement using electron beam.**Fig. 3** Comparison between the calculated and the measured vibrational temperature of N_2 at nozzle exit in air over the entire range of arcjet experiment.

collisions on vibrational relaxation: at the time of MacDermott's work, the effect of O atoms on N_2 vibration⁶ was unknown.

AEDC Arcjet Species Concentration Measurement

In addition to measuring vibrational and rotational temperatures, MacDermott et al.^{20,21} also measured in the arcjet wind tunnel concentrations of O, N, N_2 , O_2 , and NO using a mass-spectrometer. In Fig. 4, the mole fractions calculated by the NOZNT code are compared with the experimental data for the case $p_s = 5$ atm and $H = 9.67$ MJ/kg. The error bars in the figure represent the extent of the scatter in the experimental data. As seen in the figure, the calculated species mole fractions for N_2 , O_2 , O, and NO undergo a freezing process, as predicted by the theory. Also, their exit values agree fairly well with the experimental data. However, the mole fraction of N undergoes a peculiar variation. Instead of monotonically decreasing, it increases slightly beyond $x = 0.3$ m. Although not perceptible in this plot, the O fraction decreases slightly in the region where N fraction increases. Examination of the forward and reverse rates of all reactions reveals that the behaviors of O and N seen here are caused by the multitemperature effect on the NO exchange reactions, reactions (2) and (3). Because the forward reaction is (assumed to be) determined mostly by $T_f = T_e$ (see Table 1) while the reverse reaction is by $T_r = T$, the reaction proceeds from left to right in the downstream region. This causes a decrease in O fraction and an increase in N fraction.

Although not shown, the calculated exit values of O and N fractions are seen to be affected sensitively by the choice of T_f , given by Eqs. (4) and (5), for reactions (2) and (3). The less weight on T_e and the more weight on T_r , the higher becomes the O fraction and the lower becomes the N fraction. The choice made in Eqs. (4) and (5) must be adhered to in order to numerically reproduce the experimental data.

In Fig. 5, a comparison is made on the nozzle exit species mole fractions among the three different methods for flow calculation for the case considered: the present (NOZNT) method, the one-temperature nonequilibrium calculation (NOZ1T) using the present rate coefficients, and the one-temperature calculation using the NENZF rate coefficients. As seen here, the one-temperature calculations overestimate O fractions and severely underestimate N fractions. The use of NENZF rate coefficients results in a greater discrepancy from the measured values than the present rate coefficient values.

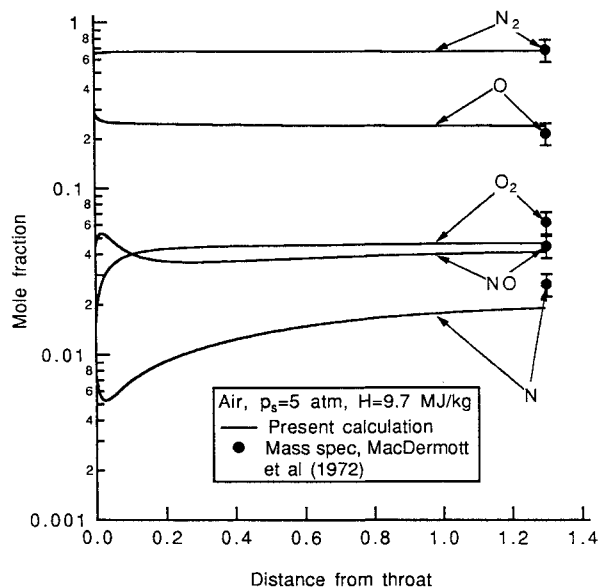


Fig. 4 Comparison between the calculated and the measured species concentrations along nozzle in air in an arcjet wind tunnel; measurement using mass spectrometer.

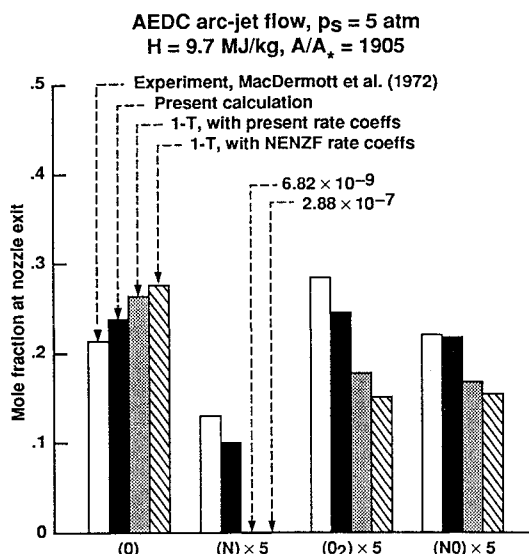


Fig. 5 Comparison between the measured species concentrations at nozzle exit and those calculated using different methods for arcjet wind-tunnel experiment.

In Figs. 6a–6c, the calculated nozzle exit species mole fractions are compared with the measured values over the tested range. The values for N, O, and NO are listed also in Table 2. The one-temperature calculations shown as dash curves in the figures are taken from the work of MacDermott et al.²⁰ Although not shown, the one-temperature calculation using NENZF rate coefficient reproduces the dash curve fairly closely, except for species N. Calculation with NENZF rate coefficients results in N-concentration values much smaller than MacDermott's. The present method gives results that agree fairly well with the experimental data over the entire tested range. The one-temperature calculation always overestimates O fraction and severely underestimates N fraction, as seen in Fig. 5.

Discussion

The observed agreement between the calculated vibrational temperatures and the values measured in arcjet flows is an evidence that the basic vibrational relaxation model of Sharma and his associates^{15,16} used in the present work, which states that vibrational relaxation in an expanding flow occurs at the same rate as behind a shock wave, is correct, and that the apparent fast vibrational relaxation in a nozzle^{7,8} is caused by the presence of greater concentration of atomic oxygen there than behind a shock wave.

Howard et al.¹⁴ measured the average vibrational temperature of NO across a wind-tunnel nozzle flow. They also made nonequilibrium calculation of the vibrational temperature. They reported that the measured vibrational temperatures are slightly lower than the calculated values, e.g., 899 K compared to 1100 K for run R3B4. This set of data was not studied in the present work because of the uncertainty introduced by the boundary layer. The outer region of a boundary layer in a hypersonic environment is much hotter than the freestream due to recovery of flow kinetic energy. The phenomenon tends to raise the measured average vibrational temperature. Therefore, the vibrational temperatures in the core of the nozzle flow in the experiment of Howard et al. are believed to be less than those measured. According to the present calculation, the NO's vibrational temperature is only 412 K for run R3B4.

Figure 5 shows that there still exists a discernible discrepancy between the present model and the experimental data on species concentrations. Calculations show that better agreement can be obtained if the electronic temperature affecting the NO exchange rates, Eqs. (4) and (5), i.e., the temperature corresponding to the concentration of the 1D

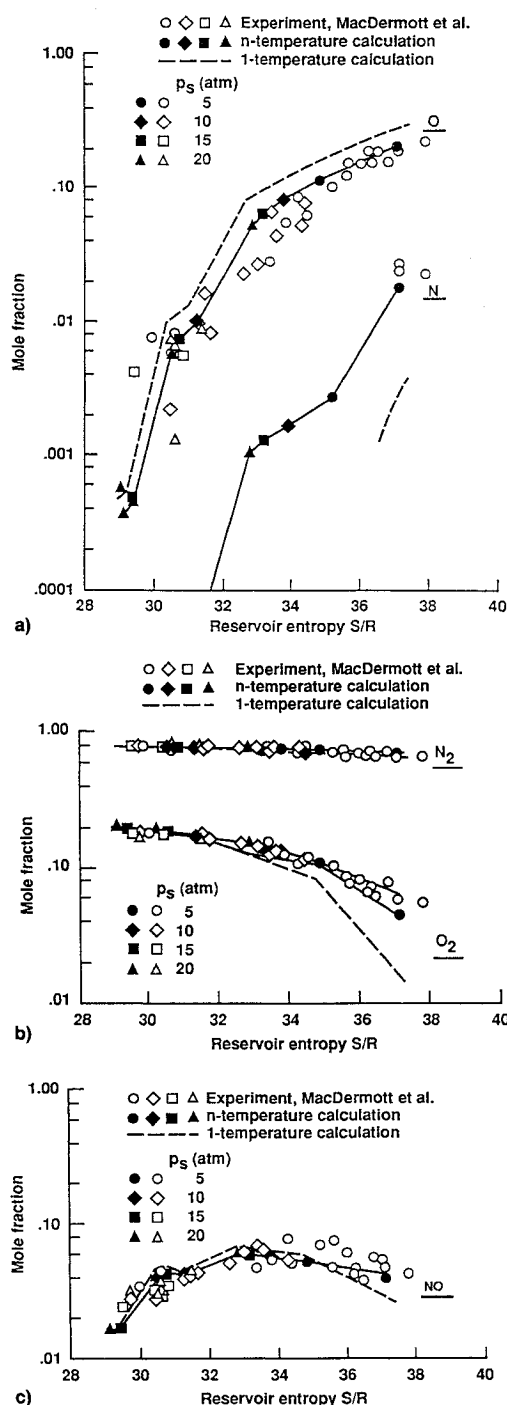


Fig. 6 Comparison between the measured species concentrations at nozzle exit and those calculated using the different methods for the entire range of arcjet wind-tunnel experiment: a) N and O, b) N_2 and O_2 , and c) NO.

state of O atoms, is assumed to be higher than that given by the present model. Common sense would say that the T_f given by Eqs. (4) and (5) depend too strongly on T_e , a T_f with more equal weights on T_e , T_v , and T would seem intuitively more appropriate. If the electronic temperature for $O(^1D)$ is indeed higher than that given by the present model, then a T_f with a more equal weight on these three temperatures could successfully reproduce the experimental data.

Figure 5 indicates that measured electronic temperature of NO $A^2\Sigma^+$ state is higher than assumed in the model. On the other hand, Ref. 28 shows that the electronic temperature of the NO $B^2\Pi$ state is lower than that of the $A^2\Sigma^+$ state. These clues lead to the suspicion that there is no common electronic temperature among the different electronic states of a species,

not to mention among different species. This means that the assumption of electronic temperature being equal to electron temperature may not be valid, and that the $O(^1D)$ temperature could be indeed higher than that given by the present method. Correctly modeling this problem is left for the future.

It is to be noted that an attempt had been made in Ref. 43 to compare the results of the calculation by the NOZNT code with the experimental data taken in shock tunnels.^{8,24-26} It was shown therein that the measured vibrational and electron temperatures are lower than calculated by NOZNT. Reference 43 attributes the difference between the experiment and the calculation to the impurities, such as iron or sodium, in the shock-tunnel flow. An alternative explanation of the discrepancy may be that the lower-state vibrational temperature, to which the line-reversal temperature⁸ and electron temperature²⁴⁻²⁶ tend to be tied, could be substantially lower than the average (energy-averaged) vibrational temperature¹⁸ calculated in NOZNT in the shock-tunnel test cases because of the Treanor distribution (see Introduction). The impact of the Treanor distribution must be accounted for in order to correctly model the shock-tunnel cases. This task is left for the future.

Finally, one must recognize that carrying five or more temperatures in calculation would strain multidimensional calculations considerably. One would hope that there would be a simpler model requiring fewer than five temperatures, and yet correctly accounting for energies in different modes at least grossly. Whether such a model is possible remains to be investigated in the future.

Conclusions

Using the NOZNT code, it is possible to numerically approximately reproduce the existing sets of experimental data taken in arcjet wind tunnels. The magnitudes of various temperatures satisfy the relationships $T_v(N_2) > T_v(O_2) > T_v(NO) > T$, and $T_e > T_v(N_2)$. Vibrational relaxation in an expanding flow occurs at the same rate as behind a shock wave as concluded by Sharma et al.,¹⁵ but appears faster only because an expanding flow contains atomic oxygen in a greater concentration. Concentration of atomic oxygen is less, and that of atomic nitrogen is greater at the nozzle exit than those calculated by the conventional one-temperature model, because of the enhanced NO exchange reactions resulting from the elevated T_e . Uncertainty still exists about the behavior of electronic excitation temperature and the extent it affects the concentration of atomic oxygen at nozzle exit.

Acknowledgments

The support for S.H.L. by NASA Grant NCC2-420 is gratefully acknowledged. The authors wish to express their sincere thanks to Dikran S. Babikian for debugging and correcting the errors in the NOZNT code.

References

- Stollery, J. L., and Park, C., "Computer Solutions to the Problem of Vibrational Relaxation in Hypersonic Nozzle Flows," *Journal of Fluid Mechanics*, Vol. 19, Pt. 1, Jan. 1964, pp. 113-123.
- Millikan, R. C., and White, D. R., "Systematics of Vibrational Relaxation," *Journal of Chemical Physics*, Vol. 139, No. 12, 1963, pp. 34-43.
- Wray, K., "Shock-Tube Study of the Vibrational Relaxation of Nitric Oxide," *Journal of Chemical Physics*, Vol. 36, No. 10, 1962, pp. 2597-2603.
- Kiefer, J. H., and Lutz, R. W., "The Effect of Oxygen Atoms on the Vibrational Relaxation of Oxygen," *Proceedings of the 11th Symposium (International) on Combustion*, The Combustion Inst., Pittsburgh, PA, 1967, pp. 67-76.
- Center, R. E., "Vibrational Relaxation of Carbon Monoxide and Carbon Dioxide by Atomic Oxygen," *Proceedings of the 9th International Symposium on Shock Tubes and Waves*, edited by D. Bershafer and W. Griffith, Stanford Univ. Press, Stanford, CA, 1973, pp. 383-394.

- ⁶Eckstrom, D. L., "Vibrational Relaxation of Shock-Heated N_2 by Atomic Oxygen Using the IR Tracer Method," *Journal of Chemical Physics*, Vol. 59, No. 6, 1973, pp. 2787–2795.
- ⁷Hurle, I. R., "Nonequilibrium Flows with Special Reference to the Nozzle-Flow Problem," *Proceedings of the 8th International Shock Tube Symposium*, Chapman and Hall, London, 1971, pp. 3/1–3/37.
- ⁸Hurle, I. R., Russo, A. L., and Hall, J. G., "Spectroscopic Studies of Vibrational Nonequilibrium in Supersonic Nozzle Flows," *Journal of Chemical Physics*, Vol. 40, No. 8, 1964, pp. 2076–2089.
- ⁹McLaren, T. I., and Appleton, J. P., "Vibrational Relaxation Measurements of Carbon Monoxide in a Shock-Tube Expansion Wave," *Journal of Chemical Physics*, Vol. 53, No. 7, 1970, pp. 2850–2857.
- ¹⁰Blom, A. P., Bray, K. N. C., and Pratt, N. H., "Rapid Vibrational De-Excitation Influenced by Gasdynamic Coupling," *Astrodynamica Acta*, Vol. 15, Nos. 5 and 6, 1970, pp. 487–494.
- ¹¹Von Rosenberg, C. W., Jr., Taylor, R. L., and Teare, J. D., "Vibrational Relaxation of CO in Nonequilibrium Nozzle Flow," *Journal of Chemical Physics*, Vol. 48, No. 12, 1968, pp. 5731–5733.
- ¹²Ruffin, S. M., and Park, C., "Vibrational Relaxation of Anharmonic Oscillators in Expanding Flows," AIAA Paper 92-0806, Jan. 1992.
- ¹³MacDermott, W. N., and Marshall, J. G., "Nonequilibrium Nozzle Expansions of Partially Dissociated Air: A Comparison of Theory and Electron-Beam Experiments," Arnold Engineering Development Center, AEDC-TR-69-66, Tullahoma, TN, July 1969.
- ¹⁴Howard, R. P., Dietz, K. L., McGregor, W. K., and Limbaugh, C. C., "Nonintrusive Nitric Oxide Density Measurements in the Effluent of Core-Heated Airstreams," AIAA Paper 90-1478, June 1990.
- ¹⁵Sharma, S., Ruffin, S. M., Gillespie, W. D., and Meyer, S. A., "Nonequilibrium Vibrational Population Measurements in an Expanding Flow Using Spontaneous Raman Spectroscopy," AIAA Paper 92-2855, July 1992.
- ¹⁶Gillespie, W. D., Bershader, D., Sharma, S. P., and Ruffin, S. M., "Raman Scattering Measurements of Vibrational and Rotational Distributions in Expanding Nitrogen," AIAA Paper 93-0274, Jan. 1993.
- ¹⁷Treanor, C. E., Rich, J. W., and Rehm, R. G., "Vibrational Relaxation of Anharmonic Oscillators with Exchange-Dominated Collisions," *Journal of Chemical Physics*, Vol. 48, No. 4, 1968, pp. 1798–1807.
- ¹⁸Ruffin, S. M., "Vibrational Energy Transfer of Diatomic Gases in Hypersonic Expanding Flows," Ph.D. Dissertation, Stanford Univ., Dept. of Aeronautics and Astronautics, Stanford, CA, June 1993.
- ¹⁹Bray, K. N. C., "Atomic Recombination in a Hypersonic Wind-Tunnel Nozzle," *Journal of Fluid Mechanics*, Vol. 6, Pt. 1, July 1959, pp. 1–32.
- ²⁰MacDermott, W. N., and Dix, R. E., "Final Results of On-Line Spectrometric Analysis of Nonequilibrium Airflows," Arnold Engineering Development Center, AEDC-TR-71-23, Tullahoma, TN, Feb. 1971.
- ²¹MacDermott, W. N., and Dix, R. E., "Mass Spectrometric Analysis of Nonequilibrium Airflows," *AIAA Journal*, Vol. 10, No. 4, 1972, pp. 494–498.
- ²²Stalker, R. J., and McIntosh, M. K., "Hypersonic Nozzle Flow of Air with High Initial Dissociation Levels," *Journal of Fluid Mechanics*, Vol. 58, Pt. 4, May 1973, pp. 749–761.
- ²³Spurk, J. H., "Experimental and Numerical Nonequilibrium Flow Studies," *AIAA Journal*, Vol. 8, No. 6, 1970, pp. 1039–1045.
- ²⁴Dunn, M. G., and Lordi, J. A., "Measurement of Electron Temperature and Number Density in Shock Tunnel Flows, Part 2. NO^+ + e Dissociative Recombination Rate in Air," *AIAA Journal*, Vol. 7, No. 11, 1969, pp. 2099–2104.
- ²⁵Dunn, M. G., and Lordi, J. A., "Measurement of $N_2^+ + e$ Dissociative Recombination in Expanding Nitrogen Flows," *AIAA Journal*, Vol. 8, No. 2, 1970, pp. 339–345.
- ²⁶Dunn, M. G., and Lordi, J. A., "Measurement of $O_2^+ + e$ Dissociative Recombination in Expanding Oxygen Flows," *AIAA Journal*, Vol. 8, No. 4, 1970, pp. 614–618.
- ²⁷Lordi, J. A., and Dunn, M. G., "Sources of Electron Energy in Weakly Ionized Expansions of Nitrogen," Cornell Aeronautical Lab., Rept. AI-2187-A-16, Buffalo, NY, Aug. 1969.
- ²⁸Gopaul, K. J. M., Babikian, S. D., and Park, C., "Measurement and Analysis of NO Radiation in an Arc-Jet Flow," AIAA Paper 93-2800, July 1993.
- ²⁹Park, C., "Estimation of Excitation Energy of Diatomic Molecules in Expanding Nonequilibrium Flows," AIAA Paper 92-0805, Jan. 1992.
- ³⁰Park, C., *Nonequilibrium Hypersonic Aerothermodynamics*, Wiley, New York, 1990.
- ³¹Lordi, J. A., Mates, R. E., and Moselle, J. R., "Computer Program for the Numerical Solution of Nonequilibrium Expansions of Reacting Gas Mixtures," NASA CR-472, 1972.
- ³²Lomax, H., "Stable Implicit and Explicit Numerical Methods for Integrating Quasi-Linear Differential Equations with Parasitic-Stiff and Parasitic-Saddle Eigenvalues," NASA TN D-4703, July 1968.
- ³³Oldenberg, R., Chinitz, W., Friedman, M., Jaffe, R., Jachimowski, C., Rabinowitz, M., and Schott, G., "Hypersonic Combustion Kinetics: Status Report of the Rate Constant Committee, NASP High Speed Propulsion Technology Team," NASP Rate Constant Committee, NASP TM-1107, 1990.
- ³⁴Rawlins, W. T., and Fraser, M. E., "Branching Ratios for Infrared Vibrational Emission for $NO(X^2\Pi, v' = 2-13)$," *Journal of Chemical Physics*, Vol. 96, No. 10, 1992, pp. 7555–7563.
- ³⁵Hanson, R. K., and Salimian, S., "Survey of Rate Constants in the N/H/O System," *Combustion Chemistry*, edited by W. C. Gardiner Jr., Springer-Verlag, New York, 1984, pp. 361–421.
- ³⁶Park, C., "Review of Chemical-Kinetic Problems of Future NASA Missions, I: Earth Entries," *Journal of Thermophysics and Heat Transfer*, Vol. 7, No. 3, 1993, pp. 385–398.
- ³⁷Taylor, R. L., Camac, M., and Feinberg, R. M., "Measurements of Vibration-Vibration Energy Coupling in Gas Mixtures," *Proceedings of the 11th Symposium (International) on Combustion*, The Combustion Inst., Pittsburgh, PA, 1967, pp. 49–65.
- ³⁸Lee, J. H., "Electron-Impact Vibrational Relaxation in High-Temperature Nitrogen," AIAA Paper 92-0807, Jan. 1992.
- ³⁹Ali, A. W., "Excitation and Ionization Cross-Sections for Electron Beam and Microwave Energy Deposition in Air," Naval Research Lab., NRL Memorandum Rept. 459780, Washington, DC, 1982.
- ⁴⁰MacDermott, W. N., Horn, D. D., and Fisher, C. J., "Flow Contamination and Flow Quality in Arc Heaters Used for Hypersonic Testing," AIAA Paper 92-4028, July 1992.
- ⁴¹Palumbo, G., Craig, R., and Carrasco, A., "Spectral Measurements of Shock Layer Radiation in an Arc-Jet Wind Tunnel," 39th International Instrumentation Symposium, Albuquerque, NM, May 1993.
- ⁴²Dunn, M. G., "Measurement of $C^+ + e^- + e^-$ and $CO^+ + e^-$ Recombination in Carbon Monoxide Flows," *AIAA Journal*, Vol. 9, No. 11, 1971, pp. 2184–2191.
- ⁴³Park, C., and Lee, S. H., "Validation of Multi-Temperature Nozzle Flow Code NOZNT," AIAA Paper 93-2862, July 1993.